Multiple Quasi Equilibria of the ITCZ and the Origin of Monsoon Onset. Part II: Rotational ITCZ Attractors

Winston C. Chao

Laboratory for Atmospheres, NASA Goddard Space Flight Center, Greenbelt, Maryland

Baode Chen

GEST Center, University of Maryland, Baltimore County, Baltimore, Maryland

ABSTRACT

Chao's numerical and theoretical work on multiple quasi equilibria of the intertropical convergence zone (ITCZ) and the origin of monsoon onset is extended to solve two additional puzzles. One is the highly nonlinear dependence on latitude of the "force" acting on the ITCZ due to the earth's rotation, which makes the multiple quasi equilibria of the ITCZ and monsoon onset possible. The other is the dramatic difference in such dependence when different cumulus parameterization schemes are used in a model. Such a difference can lead to a switch between a single ITCZ at the equator and a double ITCZ, when a different cumulus parameterization scheme is used. Sometimes one of the double ITCZ can diminish and only the other remains strong, but still this can mean different latitudinal locations for the single ITCZ.

A single idea based on two off-equator attractors for the ITCZ symmetric with respect to the equator, due to the earth's rotation, and the dependence of the strength and size of these attractors on the cumulus parameterization scheme solves both puzzles. The origin of these rotational attractors, explained in Part I, is further discussed. Each attractor exerts on the ITCZ a force of simple shape in latitude; but the sum gives a shape highly varying in latitude. Also the strength and the domain of influence of each attractor vary when change is made in the cumulus parameterization. This gives rise to the high sensitivity of the force shape to cumulus parameterization. Numerical results, of experiments using Goddard's GEOS GCM, supporting this idea are presented. It is also found that the model results are sensitive to changes outside of the cumulus parameterization. The significance of this study to El Niño forecast and to tropical forecast in general is discussed.

1. Introduction

Through various specially designed numerical experiments with an aquaplanet general circulation model (GCM) and theoretical arguments, in Part I of this paper Chao (2000, hereafter C00) showed the existence of multiple quasi equilibria of the intertropical convergence zone (ITCZ). He also showed that monsoon onset could be interpreted as an abrupt transition between the quasi equilibria of the ITCZ. He further showed that the origin of these quasi equilibria is related to two different types of attraction (or, "forces" as called in C00) pulling the ITCZ in opposite directions. One type of attraction on the ITCZ is due to the earth's rotation, which pulls the ITCZ toward the equator or two equatorial latitudes symmetric with respect to the equator depending on the choice of convection scheme, and the other due to the peak of the sea surface temperature (SST, which is given in the experiments as a Gaussian profile in latitude and

is uniform in longitude), which pulls the ITCZ toward a latitude just poleward of the SST peak. The strength of the attraction due to the earth's rotation has a highly nonlinear dependence on the latitude and that due to the SST peak has a linear (at least in a relative sense; see C00 for discussion) dependence on the latitude. Figure 1 (same as Fig. 8a of C00) shows these two types of attraction when Manabe's moist convective adjustment (MCA) scheme is used in the model. Curve R (positive means southward) is the attraction due to the earth's rotation and line S (positive means northward) is the attraction due to SST peak when the SST peak is just south of the latitude where line S intersects the x axis. Line S intersects curve R at three places. These are the quasi equilibria; the outer two are stable and are the two possible locations for the ITCZ. When the SST peak is close to the equator, or when line S is replaced by line S2, there is only one quasi equilibrium (point A in Fig. 1) that is on the equator side of the SST peak. Point A moves poleward at a slower rate, when the SST profile is moved poleward while maintaining its Gaussian shape. As the SST profile is moved poleward, line S

Corresponding author address: Dr. Winston C. Chao, Mail Code 913, NASA Goddard Space Flight Center, Greenbelt, MD 20771.
E-mail: winston.chao@gsfc.nasa.gov
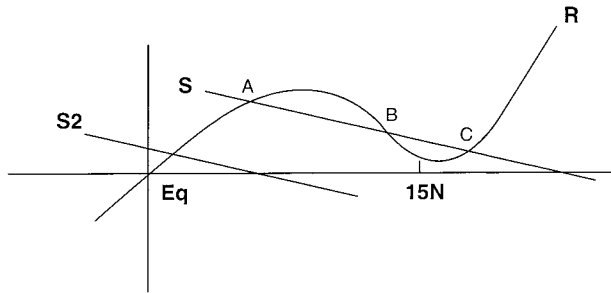
FIG. 1. Schematic diagram showing the two forces acting on the ITCZ when the Manabe scheme is used in the model. Curve R represents the force due to the earth's rotation (positive means southward). Line S represents the force due to the SST (positive means northward). The SST has a Gaussian shape in latitude and is uniform in longitude and is given in Eq. (1) of C00.

FIG. 2. Same as Fig. 1 but for RAS. RN and RS are the forces, positive being southward, due to the rotational attractors in the Northern and Southern Hemispheres, respectively. The thick curve R is for the combined forces of the two rotational attractors in the single ITCZ regime. Line S denotes the force, positive being southward, due to the SST profile when the SST peak is at the equator.

moves poleward and (more or less) keeps its slope, quasi equilibria B and C appear but the state remains at A. As the SST peak continues to gain latitude it will come to a point that point A disappears and the state (or the ITCZ), being pulled by the difference between curve R and line S, moves rapidly toward point C. Such a rapid change of latitude of the ITCZ was interpreted in C00 as monsoon onset. The shape of curve R was confirmed by experiments; see Figs. 10 and 11 of C00 and their associated discussions. As we will demonstrate in section 3, Fig. 8c of C00, the counterpart diagram when the relaxed Arakawa–Schubert scheme (Moorthe and Suarez 1992, hereafter RAS) is used should instead be represented by Fig. 2. Curve R is now represented by two curves in the lower latitude part of the Tropics and is represented by one curve in higher latitudes.

There are two important experimental facts discovered but unexplained in C00. One is the shape of curve R, or the highly nonlinear nature of the dependence of curve R on latitude. When MCA is used, curve R, shown in Fig. 1, rises from zero at the equator with the latitude, reaches a maximum at about 8° or 9°N, drops rapidly to near zero at about 14°N, and then again rises sharply northward at a rate much higher than that at the equator. It is antisymmetric with respect to the equator. It is this highly nonlinear dependence that makes the multiple quasi equilibria of the ITCZ and monsoon onset possible. The other unexplained fact is the drastic difference in the shape of curve R when different cumulus parameterization schemes are used (i.e., the different shape of curve R in Figs. 1 and 2). When RAS is used, curve R, also deduced experimentally and to be reported in section 3, has a different structure. Because of the different shape of curve R (as reported in C00), when SST is globally uniform (i.e., line S is zero), the intersects of curve R and line S (or the x axis) give a single ITCZ at the equator in the case of the Manabe scheme and a double ITCZ in the case of RAS (Fig. 1 of C00.) This feature remains when the SST takes on a Gaussian shape and its peak is not too strong (i.e., the slope of line S

is not too high) and is in the equatorial region. These are very different results.

The purpose of this paper is to investigate these two puzzles after some supplementary exposition of a few points mentioned in C00. The approach is the same as in C00, that is, theoretical arguments supported by numerical experiments. The model used, an updated version of the model used in C00, is described briefly in section 2. The change of model version is not crucial to this study and is made only to keep up with the model development effort at Goddard. Our idea for solving the two puzzles, comments, and exposition are described in section 3. Section 4 describes the supporting numerical experiments. This paper is concluded with some remarks and a brief summary in the last section.

2. Model used

The latest version of the Goddard Earth Observing System General Circulation Model version 2 (GEOS-2 GCM) is used. A 5° latitude × 4° longitude grid size and 20 levels are used with 4 levels below 850 mb. This model uses the discrete dynamics of Suarez and Takacs (1995). The RAS scheme (Moorthi and Suarez 1992) is a main feature of the model. This scheme gives almost identical time-mean results as the original Arakawa–Schubert scheme at much reduced computational cost. RAS is used in conjunction with a rain-reevaporation scheme (Sud and Molod 1988). The large-scale moist and dry convection remain the same as documented in Kalnay et al. (1983). In some experiments in this work RAS is replaced by the moist convective adjustment scheme of Manabe et al. (1965). The boundary layer and turbulence parameterization, a level 2.5 second-order closure model, is that of Helfand and Labraga (1988; 1989). The longwave radiation package is that of Chou

and Suarez (1994). The shortwave radiation package is that of Chou (1992) and Chou and Lee (1996). The prognostic cloud water parameterization of Del Genio et al. (1996) is used. Sea surface temperature, sea ice, and snow are from observations (for details see Takacs et al. 1994.) We will use only the aquaplanet version of this model with specified zonally uniform SST as in C00; thus some features of the model, such as land surface process parameterization (Koster and Suarez 1996) and gravity wave drag parameterization (Zhou et al. 1996), are not used.

3. Interpretation

C00 has shown that with temporally and globally uniform SST and solar zenith angle the model shows a single ITCZ at the equator when the Manabe scheme is used and double ITCZ at 13°S and N when RAS is used. As explained in C00 under such settings, if the earth's rotation is excluded, everywhere on the globe is the same and there is no favored location for precipitation and the time-mean precipitation should be uniform or that of Benard cell-like convection. When the earth's rotation is included, precipitation does find favored latitude due to two effects of rotation on convection. As stated in C00, the first effect is the equivalence of rotation to vertical stratification with higher rotation corresponding to greater vertical stratification (Veronis 1967). Here the rotation is that in the vertical direction; that is $\Omega \sin \phi$, where Ω is the earth's rotation rate and ϕ is the latitude. A simple way to understand this equivalence is by first noting that convection is associated with convergence at low levels and divergence at high levels. When one takes the time derivative of the divergence equation and substitutes the time derivative of the vorticity term by the vorticity equation, one finds that the second time derivative of divergence δ is related to divergence itself with a coefficient of f squared and a negative sign, that is,

$$\frac{\partial^2 \delta}{\partial t^2} = -f^2 \delta + \cdots .$$

This equation, ignoring the other terms (which do not have the f factor, assuming an f-plane situation) on the right-hand side, has the same form as the equation that governs a spring. Like a spring that resists any pressing or stretching, rotation resists any convergence or divergence, which has the equivalent effect of resisting the vertical motion associated with convection (which is associated with low-level convergence and upper-level divergence), which in turn is the same as what stratification does to convection. This gives rotation an effect equivalent to stratification. Another way to understand this effect of rotation is to consider the frequency of inertial-gravity waves σ [from Eq. (8.4.23) of Gill 1982],

$$\sigma^2 = f^2 + \alpha^2 N^2, \quad (1)$$

where f is the Coriolis parameter, α is the ratio of horizontal to vertical wavenumbers, N^2 is the Brunt–Väisälä frequency squared, which is $g\partial(\ln\theta)/\partial z$ in dry atmosphere, and θ is the potential temperature. In a saturated atmosphere N^2 is $g\partial(\ln\theta_e)/\partial z$, where θ_e is the equivalent potential temperature. The exact definition of N^2 for unsaturated atmosphere is not a concern here. Suffice it to say that, without rotation, when N^2 turns negative, convection occurs. In the presence of rotation, when N^2 is everywhere the same and turns negative, the location where σ^2 turns negative first is the equator. Since f^2 can be added to a term proportional to N^2 [in Eq. (1)], it must have an equivalent effect as the latter. Therefore, the ITCZ favors the equator because of rotation.

The second effect of rotation is, as stated in C00, that the boundary layer air converging toward the convective centers picks up sensible and latent heat from the surface and this energy intake is increased by inflow's taking a longer inward-spiraling path with higher speed (due to the azimuthal wind component) when earth's rotation, or the Coriolis force, is present. Thus this second effect favors the Poles for convection to occur. The compromise of the two effects favors locations at about 13°N and S for the aquaplanet condition when RAS is used, as determined by experiments in C00 (C00 reported 17°N and S, but longer integration shows 13°N and S). These locations can vary when the design of cumulus parameterization, boundary layer parameterization, or other aspects of the model is changed. As reported in C00 one of the double ITCZ may disappear and only a single ITCZ about 13° away from the equator remains. When MCA is used, as shown in Fig. 1 of C00 only a single ITCZ appears at the equator. This will be discussed shortly. There are also rainbands at 30°N and S and higher latitudes when MCA is used. A possible cause of these rainbands is the baroclinic instability, but this requires further investigation and is not dealt with in this paper.

Figure 1, same as Fig. 8a of C00, gives a good description of the two types of attraction on the ITCZ, due to Earth's rotation and SST peak, when MCA is used. However, Fig. 8c of C00, which described the situation when RAS is used, should be modified, since it does not describe the equatorial ITCZ period in Fig. 7 (late August to early October) or Fig. 12 of C00 well. We have repeated the experiment corresponding to Fig. 12 of C00 using the current version of the model. There are some minor changes in this new experiment that do not make any significant differences. The solar angle is fixed for an equinox condition. A condition that the boundary layer relative humidity exceeds 90% before cumulus convection is allowed is added. The model is run for 100 days with the SST peak at the equator before the SST profile, keeping its Gaussian shape, is moved linearly in time such that the peak SST is moved from the equator to 30°N in 276 days. The resulting zonally averaged precipitation as a function of time is shown in Fig. 3a. The linear line indicates the location of the
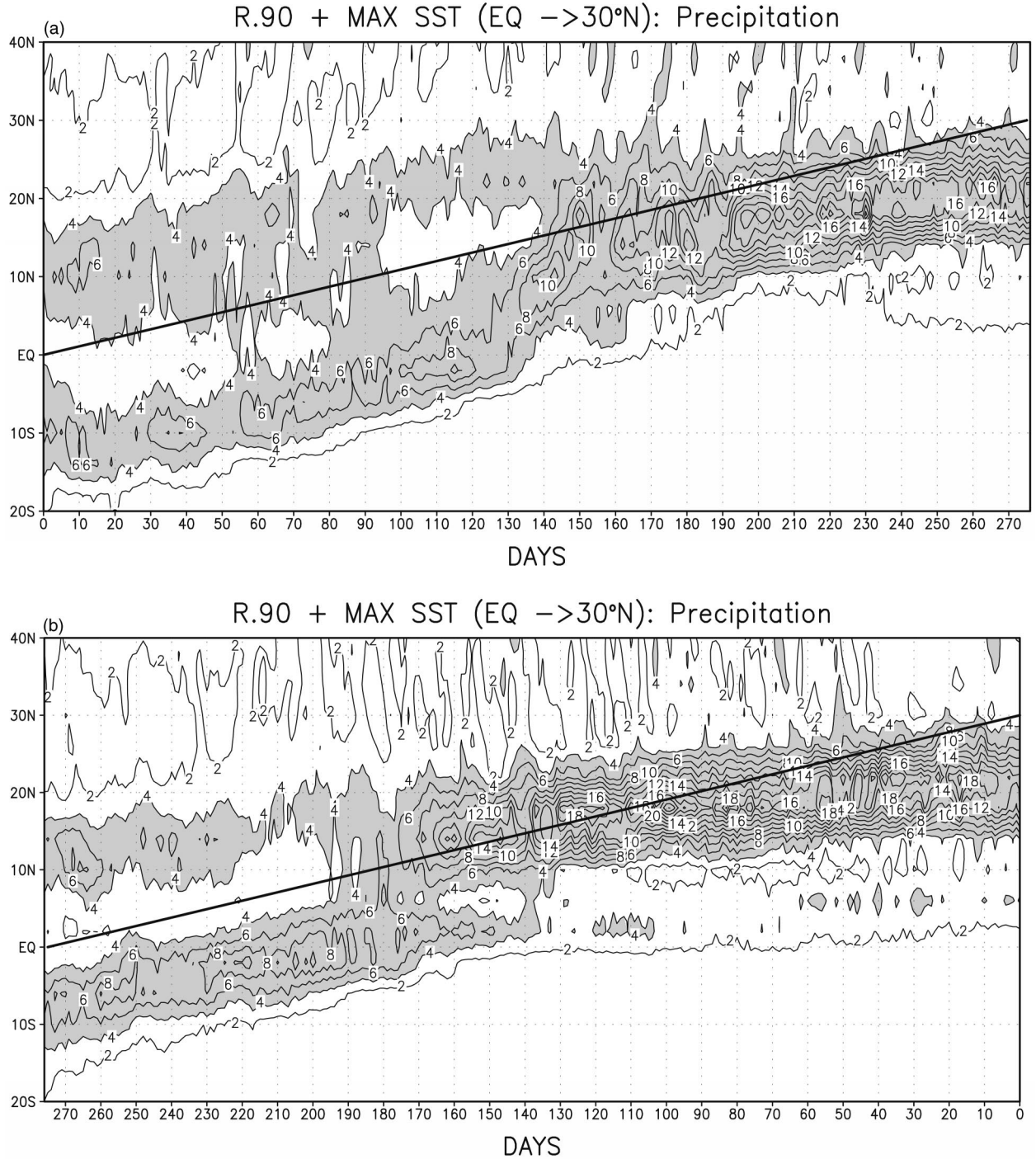
FIG. 3. Zonal-averaged precipitation (mm day^{-1}) as a function of time in an experiment using RAS and the SST profile, keeping its Gaussian shape, is moved (a) poleward and (b) equatorward. The straight line indicates the location of the SST peak. The time axis in (b) has been reversed.

SST peak. Shortly after the SST peak moves away from the equator, the southern ITCZ becomes more intense than the northern one (the reason for it is unknown) and both move northward at roughly the speed of the SST peak. The southern ITCZ, after crossing the equator, moves farther north at a much higher speed. It then merges with the northern ITCZ. After that the single ITCZ gains in intensity and moves northward at a very slow speed. Thus, there are two quasi equilibria, one has double ITCZ and the other a single ITCZ. The global

Globally Averaged Precipitation (mm/day)
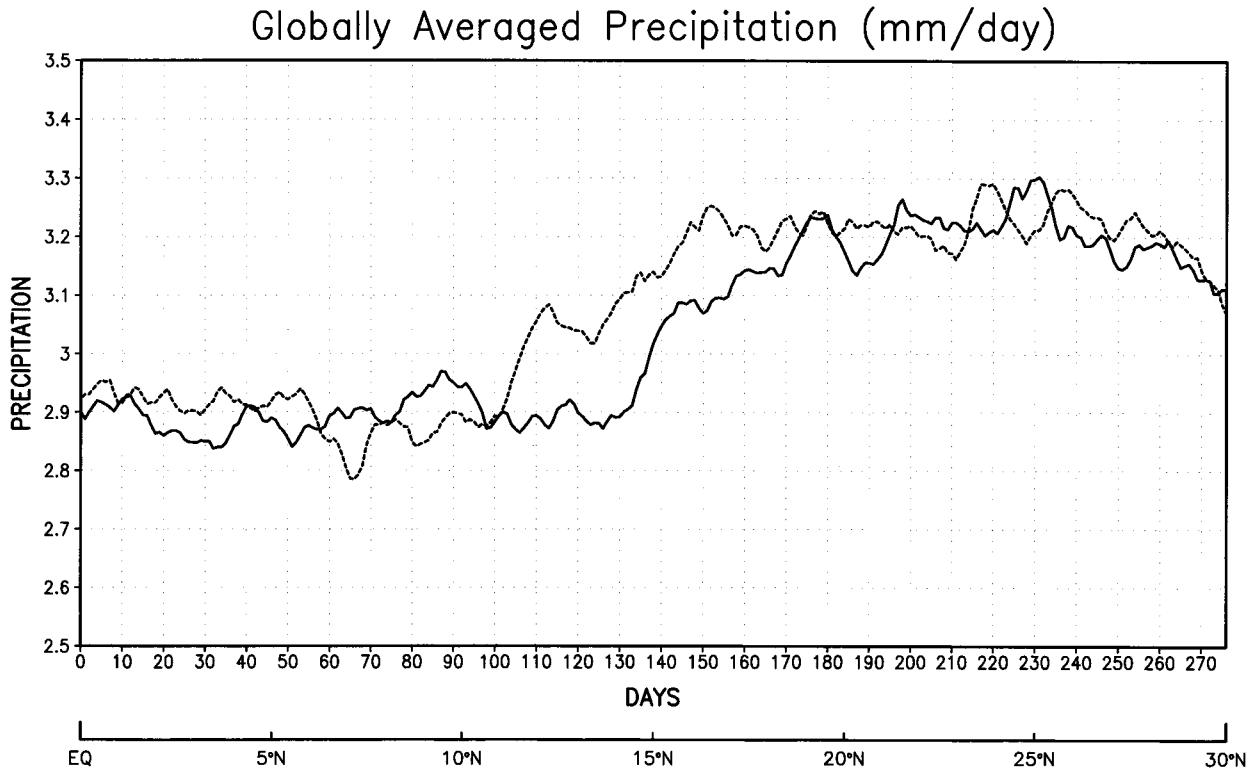
FIG. 4. The globally averaged precipitation as a function of time for the experiments described in Fig. 3. The solid line corresponds to Fig. 3a and the dashed line to Fig. 3b.

mean precipitation (Fig. 4) shows an increase of about 10% after the double ITCZ merge. Another identical experiment with the SST changed in a reversed direction, that is, the SST peak is moved from 30°N to the equator, was also conducted (Fig. 3b). In the period when the SST peak is between 10° and 15°N the two experiments give different results. This is the experimental evidence that multiple quasi equilibria exist when RAS is used. These results can be summarized by Fig. 2 (replacing Fig. 8c of C00). In Fig. 2 the straight lines represent the attraction force due to the SST profile, positive means northward. The thin curves represent the attraction due to the earth's rotation of two individual ITCZs in the double ITCZ regime and the thick curves represents the attraction due to the earth's rotation in the single ITCZ regime or it can be considered as the total attraction due to the two rotational ITCZ attractors. The centers of these two rotational ITCZ attractors are not identified in these experiments. Although their location is clearly seen in Fig. 1 of C00 where the SST is uniform, their locations may have changed due to the introduction of SST profile. Thus, the change from Fig. 8c of C00 to Fig. 2 has two components. First the peak attraction is now located much closer to the equator (but does not cross the equator). Second, the two attractors have to be treated separately until the SST peak is more than 10°–15° away from the equator.

In our investigation we have pointed out the fact that there are two types of attraction acting on the ITCZ; one due to the SST peak and the other (which can be a double attractor when RAS is used) the earth's rotation. The two types of attraction are assumed to add up to the net attraction. This additive assumption deserves some discussion. As stated in C00, if one were to do an analytic study of the net attraction (or the net force) on the ITCZ of an aquaplanet with zonally uniform SST, one would proceed to derive the governing equation of the latitudinal location of the ITCZ. This equation has the form of second time derivative of the latitudinal location of the peak of the ITCZ equal to an expression that reduces to curve R when the SST is uniform and to curve S when the Coriolis force is set to zero. If the expression contains two separate terms representing curve R and curve S, then our additive assumption is exactly right. On the other hand if the expression cannot be separated into two such terms, then the assumption is at best only approximate. We do not know at this time which of these two possibilities is the correct one. However judging from the fact that under this assumption our investigation has gone successfully (mainly because we have used the concept embedded in Fig. 1 only in a qualitative way), we can conclude that this assumption is at least approximately correct. This discussion, of course, points out the desirability of an analytic study of the ITCZ attractors.
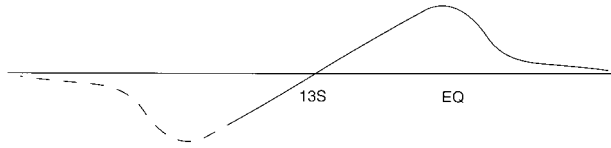
FIG. 5. The schematic shape of the attracting force due to an ITCZ attractor. The force (positive means southward) is zero at the center of the attractor and increases sinusoidally away from the center and falls exponentially after reaching a peak. The dashed line is used to remind that the force is not antisymmetric with respect to the center.

Now we are ready to deal with the two puzzles of how to explain Fig. 8a of C00 (or Fig. 1) and Fig. 2 (the replacement for Fig. 8c of C00) and why the choice of cumulus parameterization schemes can make so much of a difference. We can consider the locations of 13°N and S as the centers of two attractors pulling on the ITCZ due to the earth's rotation when the SST and the solar angle are uniform (which we name the rotational ITCZ attractors). The attraction (or the force as explained in C00) due to each attractor on the ITCZ is shown in Fig. 5 with positive values being southward. The force (or attraction) is zero at the center of the attractor and has different signs on the two sides of the center. The magnitude of the force reaches a peak at some distance away and then falls at greater distance. The rise of the force from zero at the center of the attractor is assumed to be of sinusoidal type and the fall at greater distance is assumed to be of exponential type. These are reasonable assumptions, in the sense that deductions based on these assumptions fit experimental results. Theoretically, these assumptions are reasonable because the force, due to the finite size of the attractors, has to diminish at greater distance. Although we can say that the scale of the attractors (or, the latitudinal distance from the center of the attractor to where the force is the largest) has something to do with the vigor of convection, exactly what determines it still awaits more theoretical work.

If the attractors become stronger and wider or if the centers of the attractors move closer to the equator (say, when a different cumulus parameterization scheme is used, when some parameters in the scheme are tuned, or when some features in the model outside of the cumulus parameterization scheme are changed), the force peak location can be moved to the other side of the equator. The situation can change to give curve R a shape shown in Fig. 1, which has a stable quasi equilibrium at the equator. Figure 6 shows such a combination. In other words, the two rotational ITCZ attractors away from the equator merge into one centered over the equator. In Fig. 6 the slope of curve R at the equator is the same as the slope of the force at the equator due to either attractor. The latter is smaller than the slope of the force at the center of either attractor. Due to the rapid decline of the force due to the 13°S attractor south of 13°N, at 13°N the slope of curve R is almost the same as that of the 13°N force at its center. This is
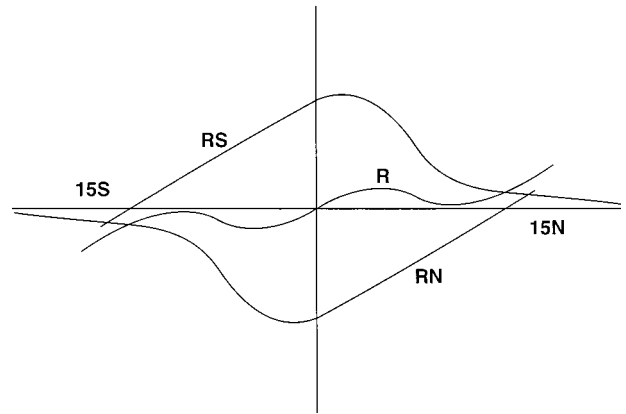
FIG. 6. The combination, R, of two rotational ITCZ attractors, RN and RS, with large domain of influence.

consistent with the experimental fact that the rise of curve R north of 13°N is greater than its rise at the equator. The sum of the two forces after reaching a peak around 7°N drops quickly poleward to give curve R a shape like what is shown in Fig. 1. Numerical experiment results will be presented in the next section to support this idea.

4. Supporting numerical experiments

According to the idea in the preceding section, it is possible to make changes in a cumulus parameterization scheme and obtain a change in the experimental outcome from one depicted by Fig. 2 to another depicted by Fig. 1 or vice versa. This will result in a change in the stable quasi equilibria, or a change between double ITCZ (or a single ITCZ away from the equator) and a single ITCZ at the equator. We will make a change in RAS, which is an addition of a condition to be met before cumulus convection is allowed to occur. The condition is that the boundary layer relative humidity has to be greater than a critical value, r_c. This condition was used by Wang and Schlesinger (1999) in a GCM to improve the simulation of the Madden–Julian oscillation. We found it also useful for our present purpose. Raising r_c gives a more intense ITCZ (because cumulus convection becomes harder to occur, and when it does occur it is more intense) and the rotational attractors become stronger and their force peaks (in absolute value) can cross the equator (starting from curve RS or RN in Fig. 2). The shape of curve R can change from that of Fig. 2 to that of Fig. 1 and correspondingly the two off-equator stable ITCZ quasi equilibria change to one at the equator.

Figure 7 shows the zonal mean precipitation averaged over the last 100 days of three 455-day experiments using RAS with uniform SST of 29°C with r_c equal to 0%, 90%, and 95%. The initial conditions are the same as those in C00 and the solar angle is the globally averaged value. In the first two experiments the curve R

RAS + Uniform SST: R.00, R.90 and R.95 Precipitation
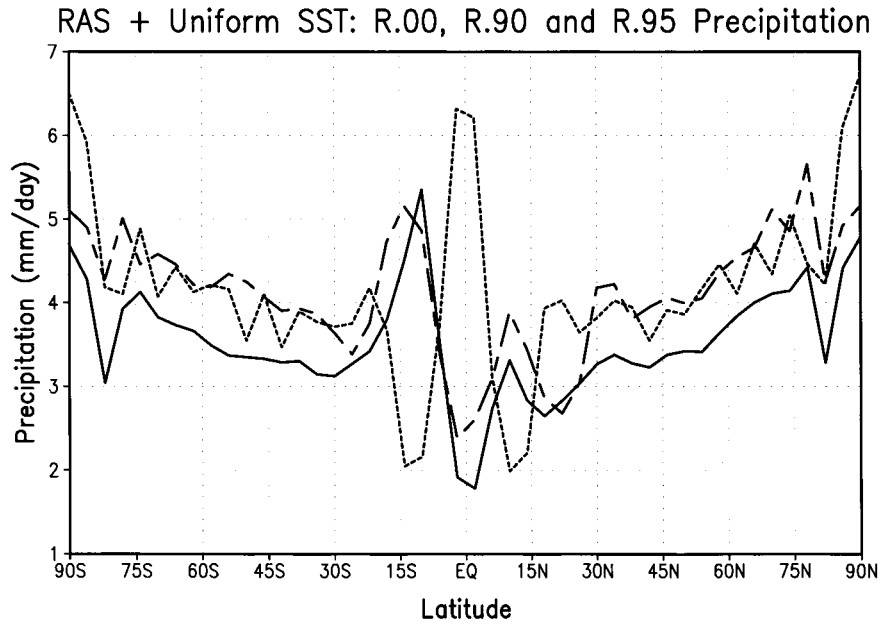
FIG. 7. Zonal mean precipitation (mm day^{-1}) averaged over the last 100 days of three 455-day experiments with uniform SST of 29°C and with the condition of boundary layer relative humidity being greater than 0% (solid), 90% (long dash), and 95% (short dash) imposed on RAS.

has the shape of Fig. 2 and the third experiment curve R has the shape of Fig. 1. Figure 8 shows the ITCZ location of an experiment with uniform SST of 29°C where RAS is used and r_c is increased from 90% to 95% linearly in 100 days after a period of 200 days with $r_c = 90\%$. The ITCZ that starts out being away from the equator switches to the equator in a short period of 30 days. Figure 9 is an identical experiment except

vc5.9a20/(R.90 -> R.95) + uniform SST
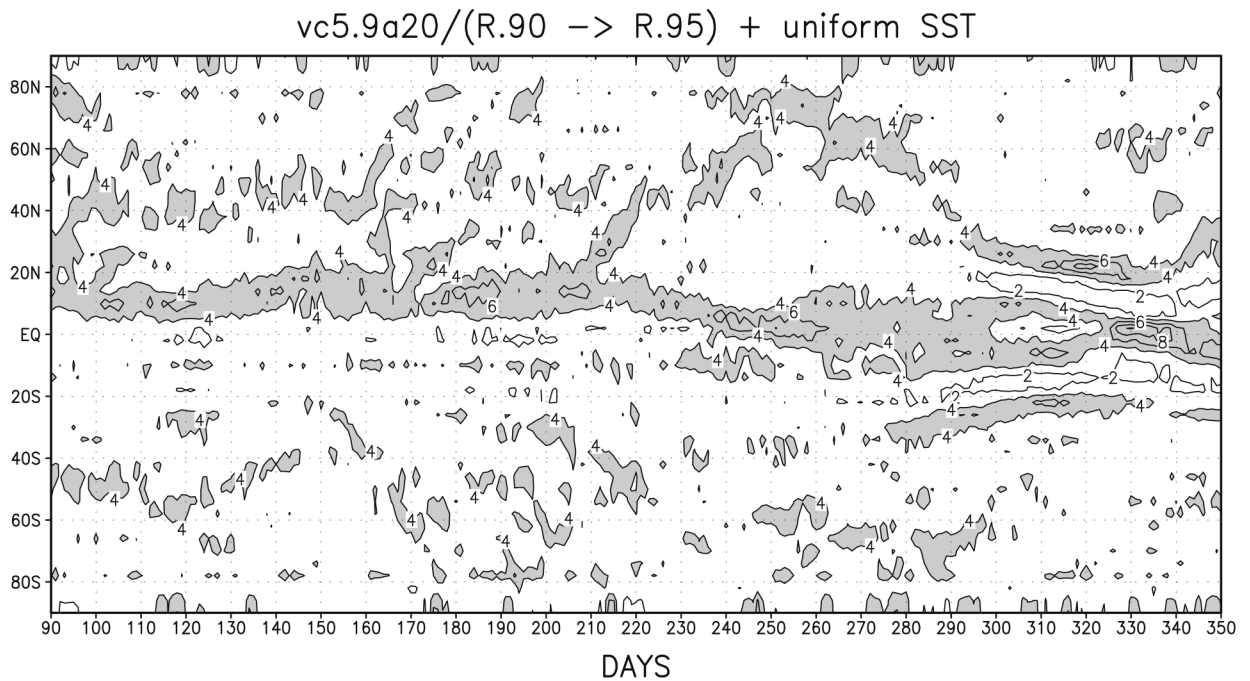
FIG. 8. Zonal mean precipitation (mm day^{-1}) of an experiment with uniform SST and solar angle using RAS and r_c is increased from 90% to 95% linearly in 100 days after a period of 200 days with $r_c = 90\%$. Here r_c is the critical relative humidity value above which cumulus convection is allowed.
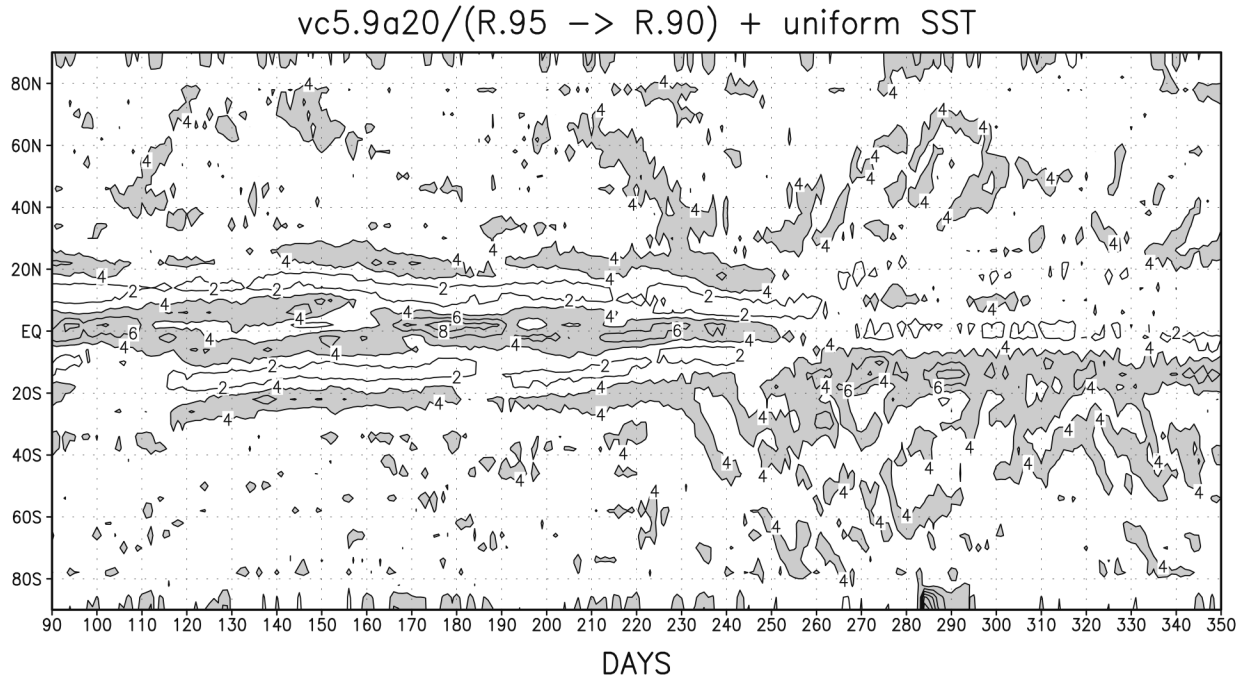
FIG. 9. Identical to Fig. 8 except the values of r_c = 90% and 95% are switched.

the r_c values of 90% and 95% are switched. The ITCZ that starts out at the equator switches away from the equator; the switch in this case is much faster, almost instantaneous around day 250. The equatorial ITCZ regime in Figs. 8 and 9 shows occasional split into double ITCZ structure (e.g., day 112–160 in Fig. 9). However this structure, in which the ITCZs are only 6° or 7° away from the equator, is distinctly different from the ITCZ in the other regime (of r_c = 90%) where the ITCZ is 13° away from the equator and exists in only one hemisphere. In the equatorial ITCZ regime there are also weaker rainbands located at 19°–23° in both hemispheres, which oscillate in time with an intraseasonal periodicity (which are reflected in the dash line in Fig. 7) and are weaker when the ITCZ at the equator becomes stronger. Although the reason for such a flow regime remains to be investigated, this result reveals the complexity and richness of the interaction between convection and large-scale circulations and the need for further refinement of our theory. The framework of this refinement is that the rotational ITCZ attractors we proposed should be considered as quasi equilibria (as stated in C00) instead of fixed point attractors. Thus there can be small oscillation in time of the location, strength, and shape of the attractors and it is these small oscillations that give rise to a variety of complex flow patterns.

The shape of curve R is revealed, as in Fig. 10 of C00, by specifying the SST as a Gaussian profile as given by Eq. (1) in C00 and moving the SST profile slowly poleward (the peak of the SST, after being fixed at the equator for 100 days, moves from the equator to 30°N linearly in 276 days) for both 90% and 95% cases.

Figures 10 and 11 (using a globally uniform solar angle equal to the global mean solar angle) show these results and reveal the shape of curve R in the two cases to be those of curve R in Figs. 1 and 2 (Figs. 12 and 10 being similar to Figs. 12 and 10 of C00 respectively). Thus besides the confirmation that RAS can be modified to give both shapes of curve R, we have made the additional discovery that the switch between the two shapes is a critical phenomenon.

Curve R, when RAS is used, can also be changed by removing surface friction. When the surface friction is removed, the boundary layer inflow direction becomes closer to the isobaric contours and the inflow takes a longer path than in the case with surface friction. As a result the second effect of rotation discussed in section 3 becomes larger and the locations of the rotational ITCZ attractors become farther away from the equator. An experiment using RAS with uniform SST and without surface friction shows such a result (Fig. 12). Figure 12 also shows the results of increasing surface friction by a factor of three. The southern ITCZ moves closer to the equator as expected, but the northern ITCZ moves away. The reason is not clear. Because the locations of the rotational ITCZ attractors (Fig. 2) are pushed farther away from the equator, when the surface friction is removed, when the Gaussian SST profile with a peak at the equator is introduced only a single ITCZ at the equator is obtained. The dashed line in Fig. 13 shows such results, which is in contrast with the case with surface friction (solid line in Fig. 13), which shows a double ITCZ.

The experience with removing surface friction in the
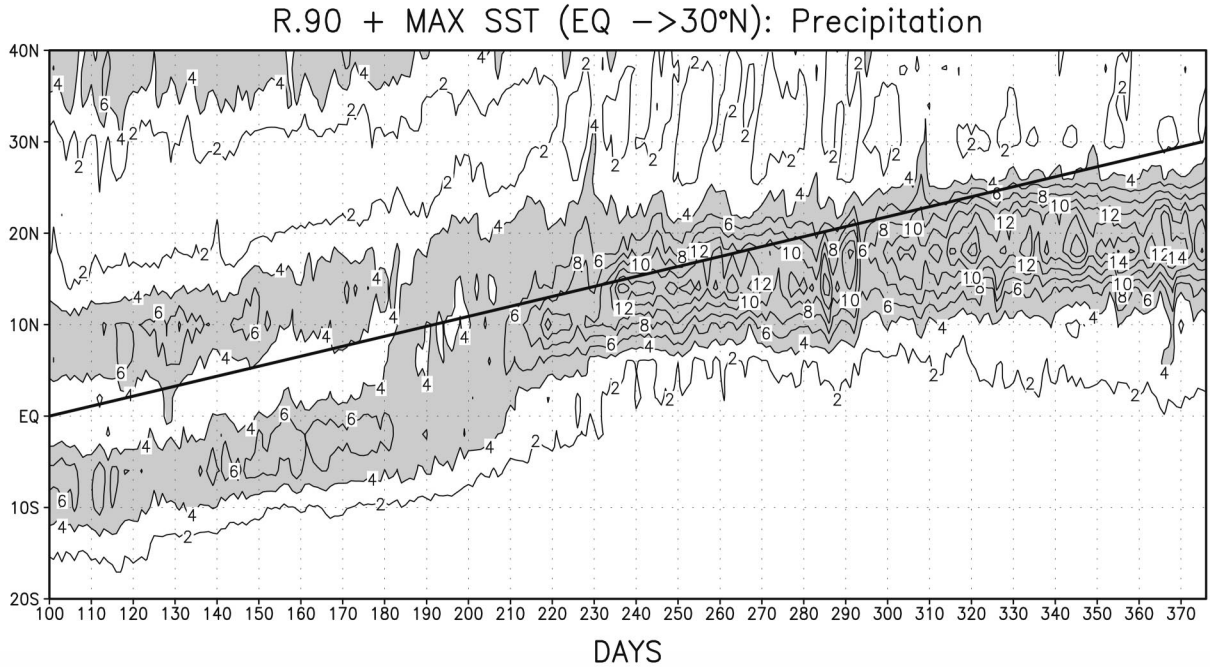
FIG. 10. Zonal mean precipitation (mm day^{-1}) in an experiment where the SST takes on a Gaussian profile and the profile is moved northward such that the SST peak moves from the equator to 30°N in 276 days. Here r_c is 90%.

RAS case suggests the possibility that the single ITCZ over the equator in the experiments using MCA can be transformed into a double ITCZ or a single ITCZ away from the equator by removing surface friction. Thus an experiment of 400 days long using MCA with uniform

SST of 29°C and without surface friction was conducted. The result (Fig. 14) still remains as a single ITCZ at the equator. However, the single ITCZ is much broader in latitudinal direction (and is occasionally split into two with peaks very close to the equator). This indicates that
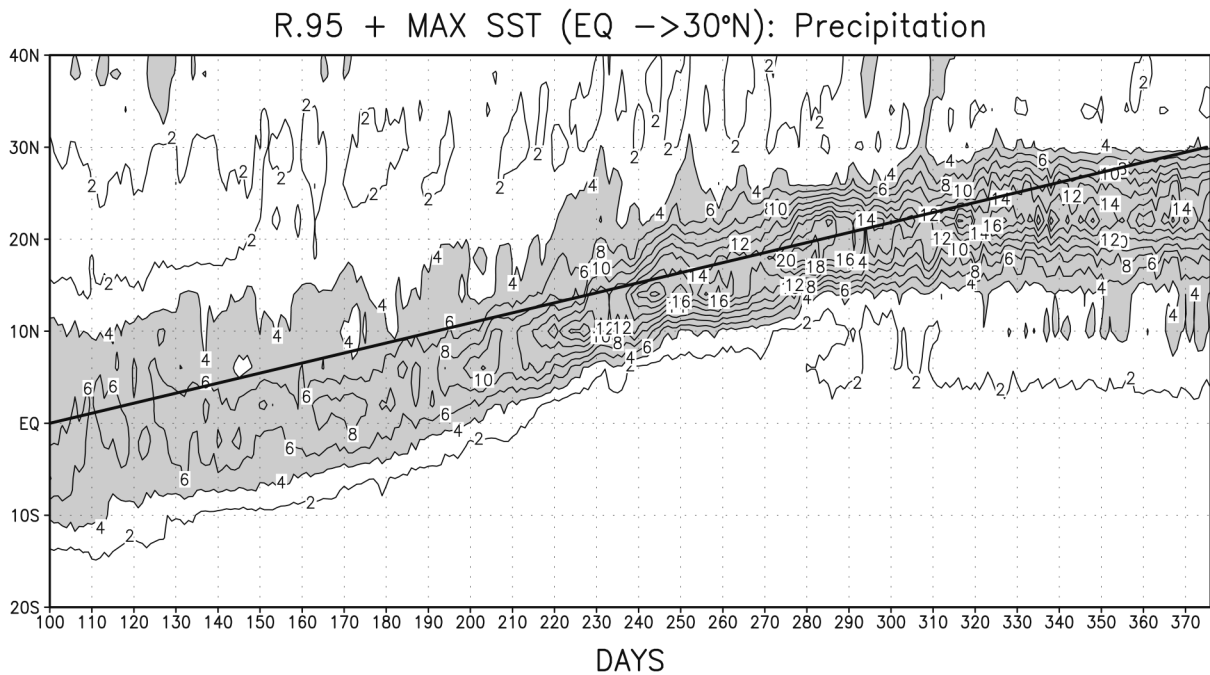
FIG. 11. Same as Fig. 10 but r_c is 95%.

w/ 3.0&1.0&0.0*sfc friction + R.00 + Uniform SST (355–455 days): Precip.
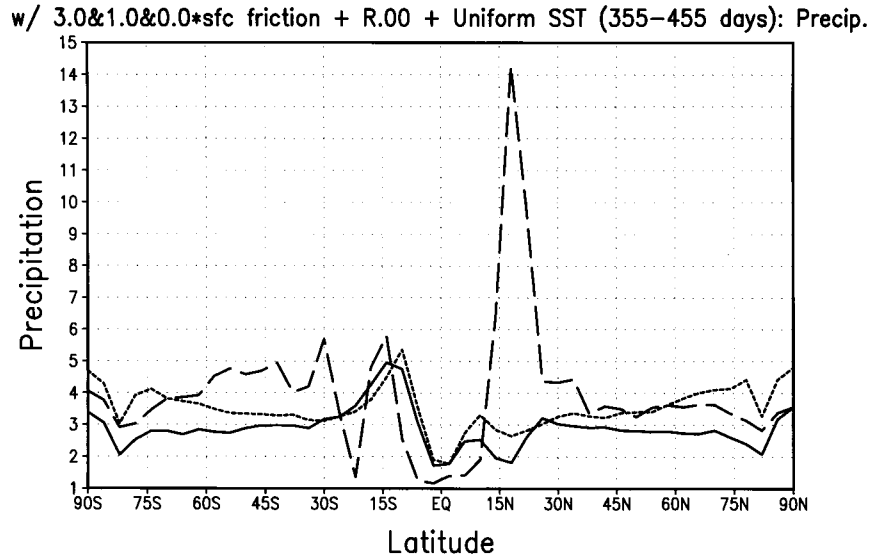
FIG. 12. Time- and zonal mean precipitation (mm day^{-1}) for experiments using RAS with no surface friction (long dash), with no change in surface friction (solid), and with a factor of three multiplied to the surface friction coefficient (short dash).

the slope of curve R at the equator has become smaller. And this smaller slope is consistent with the moving apart of the two attractors. In Fig. 6 it is obvious that the slope of R at the equator is the same of the slope of either RS or RN at the equator and if the two attractors are moved apart the slope of R at the equator becomes smaller, which gives a less sharp ITCZ over the equator. Other attempts to obtain a double ITCZ using MCA, such as changing critical relative humidity for convec-

tion to start, changing the Coriolis parameter, and changing radiative cooling rates, were also not successful.

5. Remarks and summary

Although we have demonstrated that with RAS the shape of the rotational ITCZ attractor force can be changed by tuning r_c and surface friction, other sensitive parameters in RAS need to be explored. How these pa-

w/&w/o sfc friction + MAX SST at EQ (355–455 days): Precip.
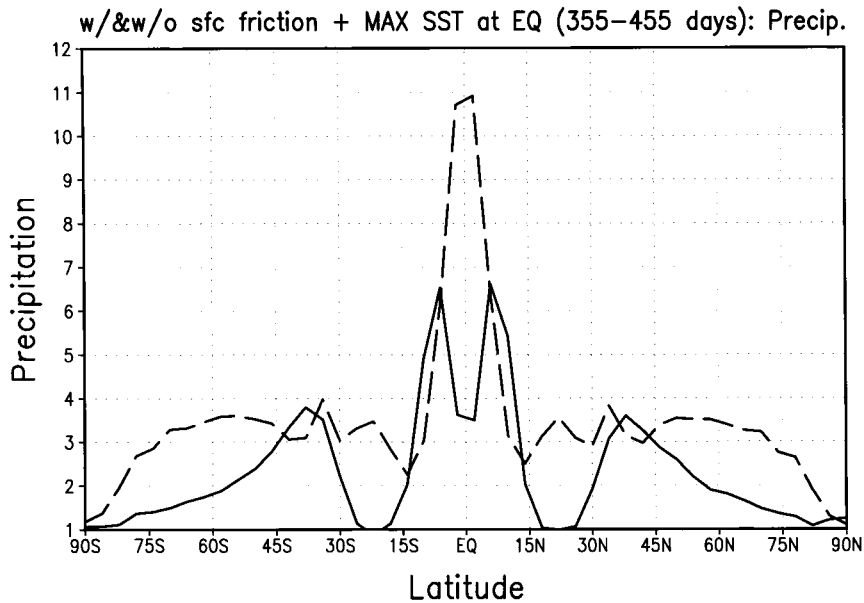
FIG. 13. Latitudinal distribution of time–zonal mean precipitation (mm day^{-1}) of RAS experiments with Gaussian SST latitudinal profile centered over the equator with (solid line) and without (dash line) surface friction.
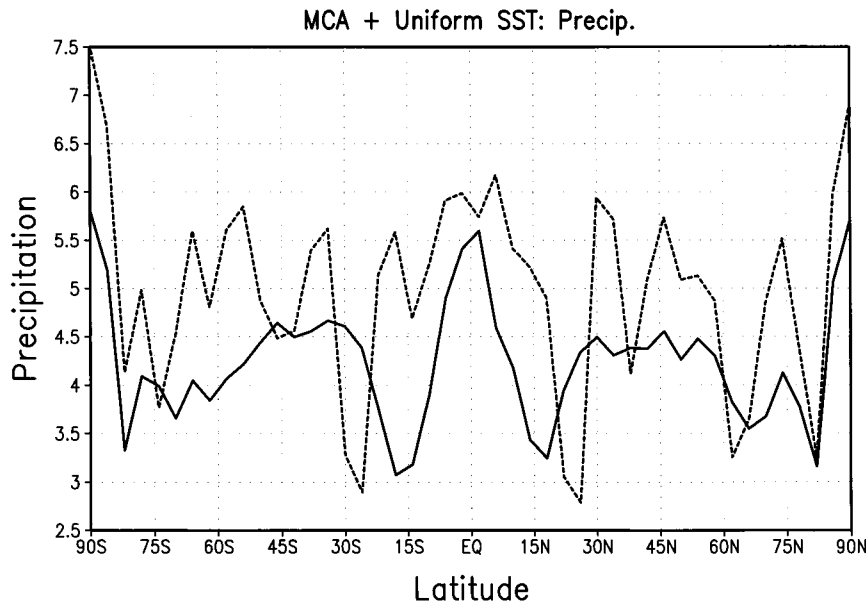
FIG. 14. Latitudinal distribution of time–zonal mean precipitation (mm day^{-1}) of MCA experiments with (solid) and without (dash line) surface friction. The SST is globally uniform.

rameters change RAS is an interesting topic. Why the attractors are wider in the case of MCA than in case of the RAS is also a question that should be investigated in the future. This may be related to the more vigorous precipitation rate in association with the individual convective cells when MCA is used, an indication that the condition for convective onset is more stringent with MCA. The eventual solution of this question involves the understanding of the interaction between cumulus heating due to a convection scheme and the large-scale circulation. This interaction involves the Coriolis force. This situation points to the need of an analytic study of the attractor force. Unfortunately such a study requires an analytic formula for cumulus parameterization, among other things, which is presently unavailable. The use of the so-called wave-CISK (conditional instability of the second kind) heating formula is not advisable (Chao and Deng 1997).

There are still more aspects to explain. When a double ITCZ is allowed, sometimes both ITCZs appear but at other times only one ITCZ occurs. What decides the choice between the two possibilities is an interesting question. When both ITCZs appear, one is stronger than the other. In Fig. 3a, when the SST peak is close to the equator the southern ITCZ is stronger than the northern one. This is another puzzle. Also in both Fig. 1 and Fig. 2 the slope of curve R has a sharp increase poleward of 17°N.

Whether a model gives a single or double ITCZ or whether a single ITCZ is located at or away from the equator has a decisive impact on the equatorial surface winds, which are crucial in the forecast of El Niño with a coupled model. Our investigation has shown the critical importance of the cumulus parameterization in sim-

ulating ITCZ and monsoon onset; therefore the importance of the cumulus parameterization to El Niño forecast or to tropical forecast in general is made more obvious through this study. The experiment we did with changing the boundary layer relative humidity required for convection with RAS is but one example of how to modify the cumulus parameterization scheme. A clear direction for future research is to explore other ways, perhaps more physically meaningful ones, to improve the performance of the cumulus parameterization scheme. We must also point out that changing cumulus parameterization is not the only way to induce change between single and double ITCZ or change in the location of a single ITCZ; changing other parts of a model can have the same effect. [For example, Sumi (1992) found that increasing horizontal resolution can change a single ITCZ along the equator into a double ITCZ straddling the equator.] However, it does appear that changes in cumulus parameterization scheme are more effective and more reasonable in inducing changes in ITCZ. The impact of modifying boundary layer parameterization in the context of tropical forecast is another worthy direction. The effect of cloud–radiation interaction on the ITCZ and monsoon onset, though appearing to be relatively minor, needs to be assessed.

In summary this investigation has solved two puzzles encountered in C00; that is, the highly nonlinear dependence of the attraction on the ITCZ due to the earth's rotation and the high sensitivity of such dependence to the cumulus parameterization scheme used in the model. A single idea based on two off-equator attractors for the ITCZ due to the earth's rotation (the rotational ITCZ attractors) and the dependence of the strength and shape of these attractors on the cumulus parameterization

scheme solves both puzzles. It is found that although the attracting force of each attractor may exhibit very simple structure, the combination of the two gives a sum highly varying in latitude and is highly varying when the cumulus parameterization scheme is modified or replaced. With the resolution of these two puzzles our interpretation for the origin of monsoon onset becomes more complete, though there are still some remaining questions. Through the circulation field associated with the ITCZ and the role of cumulus parameterization scheme in determining the location of the ITCZ, this study shows why a good cumulus parameterization scheme is crucial for a successful El Niño forecast and for a tropical forecast in general.

REFERENCES

Chao, W. C., 2000: Multiple quasi equilibria of the ITCZ and the origin of monsoon onset. *J. Atmos. Sci.,* **57,** 641–651.

——, and L. Deng, 1997: Phase-lag between deep cumulus convection and low-level convergence in tropical synoptic-scale systems. *Mon. Wea. Rev.,* **125,** 549–559.

Chou, M. D., 1992: A solar-radiation model for use in climate studies. *J. Atmos. Sci.,* **49,** 762–772.

——, and M. J. Suarez, 1994: An efficient thermal infrared radiation parameterization for use in general circulation models. NASA Tech. Memo. 104606, Vol. 3, 85 pp. [Available from NASA Goddard Space Flight Center, Greenbelt, MD 20771.]

——, and K.-T. Lee, 1996: Parameterizations for the absorption of solar radiation by water vapor and ozone. *J. Atmos. Sci.,* **53,** 1203–1208.

Del Genio, A. D., M.-S. Yao, W. Kovari, and K. K.-W. Lo, 1996: A prognostic cloud water parameterization for global climate models. *J. Climate,* **9,** 270–304.

Gill, A. E., 1982: *Atmosphere–Ocean Dynamics.* Academic Press, 662 pp.

Helfand, H. M., and J. C. Labraga, 1988: Design of a non-singular level 2.5 second-order closure model for the prediction of atmospheric turbulence. *J. Atmos. Sci.,* **45,** 113–132.

——, and ——, 1989: Reply. *J. Atmos. Sci.,* **46,** 1633–1635.

Kalnay, E., R. Balgovind, W. Chao, D. Edelmann, J. Pfaendtner, L. Takacs, and K. Takano, 1983: Documentation of the GLAS fourth-order general circulation model. Vol. 1: Model description. NASA Tech. Memo. 86064. [Available from NASA Goddard Space Flight Center, Greenbelt, MD 20771.]

Koster, R., and M. Suarez, 1996: Energy and water balance calculations in the Mosaic LSM. NASA Tech. Memo. 104606, Vol. 9, 60 pp. [Available from NASA Goddard Space Flight Center, Greenbelt, MD 20771.]

Manabe, S., J. Smagorinsky, and R. F. Strickler, 1965: Simulated climatology of a general circulation model with a hydrological cycle. *Mon. Wea. Rev.,* **93,** 769–798.

Moorthi, S., and M. J. Suarez, 1992: Relaxed Arakawa–Schubert: A parameterization of moist convection for general circulation models. *Mon. Wea. Rev.,* **120,** 978–1002.

Suarez, M. J., and L. L. Takacs, 1995: Documentation of the Aries-GEOS dynamical core: Version 2. NASA Tech. Memo. 104606, Vol. 5, 45 pp. [Available from NASA Goddard Space Flight Center, Greenbelt, MD 20771.]

Sud, Y. C., and A. Molod, 1988: The roles of dry convection, cloud–radiation feedback processes and the influence of recent improvements in the parameterization of convection in the GLA GCM. *Mon. Wea. Rev.,* **116,** 2366–2387.

Sumi, A., 1992: Pattern formation of convective activity over the aqua-planet with globally uniform sea surface temperature. *J. Meteor. Soc. Japan,* **70,** 855–876.

Takacs, L. L., A. Molod, and T. Wang, 1994: Documentation of the Goddard Earth Observing System (GEOS) General Circulation Model: Version 1. NASA Tech. Memo. 104606, Vol. 1, 100 pp. [Available from NASA Goddard Space Flight Center, Greenbelt, MD 20771.]

Veronis, G., 1967: Analogous behavior of rotating and stratified fluids. *Tellus,* **19,** 620–633.

Wang, W., and M. E. Schlesinger, 1999: The dependence on convection parameterization of the tropical intraseasonal oscillation simulated by the UIUC 11-layer atmospheric GCM. *J. Climate,* **12,** 1423–1457.

Zhou, J., Y. C. Sud, and K.-M. Lau, 1996: Impact of orographically induced gravity-wave drag in the GLA GCM. *Quart. J. Roy. Meteor. Soc.,* **122,** 903–927.